Coastal Engineering in Japan, Vol. 39, No. 2, 1996

A NUMERICAL ANALYSIS OF MULTIPLE CYLINDERS IN WAVE-CURRENT FIELD

Chung-Ren Chou [1]
Shinn-Shan Yan [2]

ABSTRACT

Effects of multiple cylinders in the wave-current field are studied by boundary element method. The potential flow field is assumed to be composed of a steady current potential and an unsteady wave potential. Dispersion relations affected by the presence of the current is used to calculate the apparent wave frequency, that means the Doppler effect is taken into consideration. The wave force on each cylinder will be presented and the wave height distributions around cylinders will be also shown.

Keywords: wave-current field, boundary element method, Doppler effect

I. INTRODUCTION

In field, waves coexist and interact with current. The complexity of the flow field increases when the dimensional effects of structures become non-negligible. Under these circumstances, the characteristics of the wave field will be severely affected. Only when all these three interacting factors were taken into consideration, a reasonable understanding of this complicated reality can be achieved.

Intensive studies on wave-current interactions have been carried out by many researchers, either theoretically, numerically or experimentally. The concept of radiation stress was first introduced by Longuet-Higgins and Steward (1961). This idea was later applied by Peregrine (1976) in the review article. Thomas (1981) studied the interaction of linear waves with current both numerically and experimentally. Effects on ship motions due to the combined wave-current actions were studied by Newman (1978). Wave diffraction and radiation by submerged body in a uniform current field were discussed by Grue and Palm (1985). Interactions between the current-wave field and two-dimensional body in the free surface were studied by Zhao and Faltinsen (1988). Baddour and Song (1990) described the interaction of linear waves and uniform collinear currents. The drift force on a slowly advancing vertical cylinder in long waves was analyzed by Eatock *et al.* (1990). Matsui *et al.* (1991) analyzed force on a vertical cylinder in a wave-current field through perturbation analysis by using potential flow theory.

Studies on wave-current interactions have usually based upon the assumption that wavelengths will be affected while their frequencies remain unchanged (see, *e.g.*,

[1]D. Eng., Professor, Dept. of Harbor and River Eng., Taiwan Ocean University, Pei-Ning Rd. 2, Keelung 202, Taiwan.
[2]B. E., Graduate Student of Doctor Course, ditto.

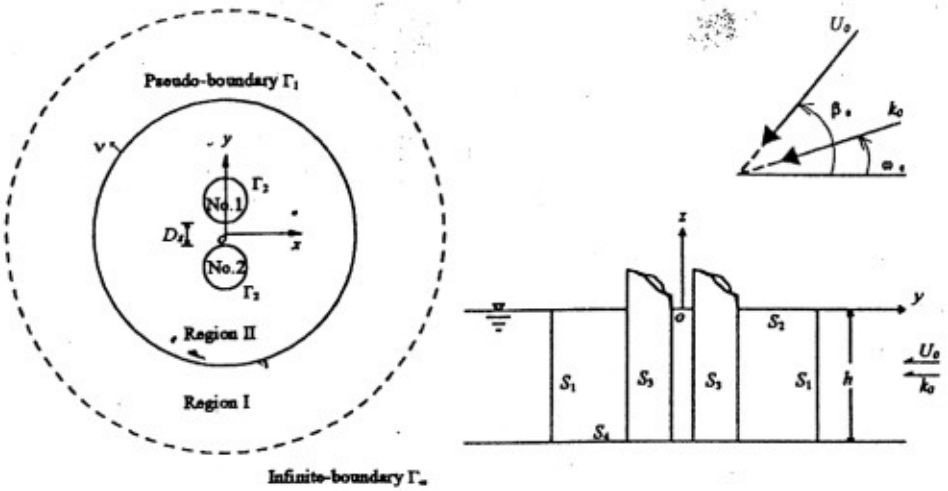

Fig. 1 Definition sketch.

Longuet-Higgins and Steward, 1961). The assumption can be questioned, since the Doppler effect states that it is the wave frequency that will be affected by current velocity. In this paper, current velocity is assumed to be small and wave is of small amplitude type that can be treated linearly. The velocity potential in wave-current field can be treated as composition of two components: a steady current potential and an unsteady wave potential. The same assumption was also used by Newman (1978), as well as Isaacson and Cheung (1993).

In this paper, it is assumed that near the cylinders, the current potential is affected by the presence of cylinders, and non-steady wave potentials are modified by the Doppler effect. In the following, variations of current velocities through the cylinders are first determined using the two-dimensional boundary element method. The dispersion relation as resulted from the Doppler effect is used to calculate the apparent wave frequencies on the water surface. Using the apparent wave frequencies, the wave potential of the wave-current-cylinders coexisting field can be estimated through the three-dimensional boundary element method. The total potential of a complicated wave-current interacting field is then recovered by combining calculated wave potential with the steady current potential.

II. THEORETICAL ANALYSIS AND NUMERICAL SCHEME

As shown in Fig. 1, the Cartesian coordinate system o-xyz is used. The x-y plane is located on the water surface with the z-axis positively upwards. Far away from the cylinders, a pseudo-boundary Γ_1 is assumed. Previous experience (Chou and Han, 1993) has shown approximately half of the length of incident wave will suffice for the present purpose. With this boundary, the domain of interest is divided into two parts. The region I is an open sea region, and the region II is a region around the cylinders.

The assumptions of the fluid being inviscid, incompressible and the flow being irrotational will be adopted here. Flow in both regions will have velocity potential

satisfying the Laplace equation. A uniform current with velocity U_o intersects the x-axis with an angle β_o in the open sea region. We consider the small amplitude waves having angular frequency σ_o ($= 2\pi/T$, where T is the period) and amplitude ζ_o, incident from the open sea at an angle of ω_o against the x-axis. Assuming further that the Froude number $F_r (= U_o/\sqrt{gh}$, where g is the gravitational acceleration, h is water depth) based upon current velocity and the wave amplitude ζ_o are all small, the velocity potential of wave-current field Φ can then be decomposed into two parts: a steady velocity potential Φ^C due to current, and a wave velocity potential Φ^W subjected to the Doppler effect,

$$\Phi = \Phi^C + \Phi^W \tag{1}$$

where both Φ^C and Φ^W satisfy the Laplace equation.

2.1 Steady Velocity Potential

(1) Current Potential in Region I

The potential for the steady current in region I is a result of potential φ^o of the current with velocity U_o incident from open sea and the potential φ^* arising from the presence of the cylinders,

$$\varphi^{(1)} = \varphi^o + \varphi^* \tag{2}$$

where $\varphi^o = -U_o(x\cos\beta_o + y\sin\beta_o)$ and the disturbed potential φ^* should satisfy the Laplace equation.

$$\frac{\partial^2\varphi^*}{\partial x^2} + \frac{\partial^2\varphi^*}{\partial y^2} = 0 \tag{3}$$

It is noted that, φ^* can be neglected far away from the cylinders. Applying Green's theorem, the potential $\varphi^*(x,y)$ in region I can be calculated by the following boundary integral equation,

$$c\,\varphi^*(x,y) = \frac{1}{2\pi}\int_{\Gamma_1}\left[\frac{\partial\varphi^*(\xi,\eta)}{\partial\nu}\ln\frac{1}{r} - \varphi^*(\xi,\eta)\frac{\partial}{\partial\nu}\left(\ln\frac{1}{r}\right)\right]ds \tag{4}$$

where $\varphi^*(\xi,\eta)$ and $\partial\varphi^*(\xi,\eta)/\partial\nu (= \overline{\varphi}^*)$ are potential and its normal derivative with ν local normal coordinate to boundary taken outwards, and $r = \sqrt{(x-\xi)^2 + (y-\eta)^2}$. The factor c is equal to unity within boundary, but will be $1/2$ on smooth boundaries.

In the numerical analysis, the boundary Γ_1, where $c = 1/2$, is discretized into N_1 segments with constant element. Equation (4) is rewritten in a matrix form as,

$$\{\varphi^*\} = \{k^*\}\{\overline{\varphi}^*\} \tag{5}$$

where

$$
\left.
\begin{aligned}
\{\varphi^*\} &= \varphi_j^* \ , \quad j = 1, 2, \cdots, N_1 \\
\{\overline{\varphi}^*\} &= \overline{\varphi}_j^* \\
\{k^*\} &= \{h^*\}^{-1}\{g^*\} \\
\{h^*\} &= h_{ij}^* \ , \quad i, j = 1, 2, \cdots, N_1 \\
\{g^*\} &= g_{ij}^* \\
h_{ij}^* &= \begin{cases} \overline{h}_{ij}^* & (i \neq j) \\ \overline{h}_{ij}^* + \dfrac{1}{2} & (i = j) \end{cases} \\
\overline{h}_{ij}^* &= \frac{1}{2\pi} \int_{\Gamma_j} \frac{\partial}{\partial \nu} \left(\ln \frac{1}{r} \right) ds \\
g_{ij}^* &= \frac{1}{2\pi} \int_{\Gamma_j} \ln \frac{1}{r} ds
\end{aligned}
\right\} \tag{6}
$$

in which $\{\varphi^*\}$ and $\{\overline{\varphi}^*\}$ are the velocity potential and its normal derivative on pseudo-boundary Γ_1, and $\{k^*\}$ is a coefficient matrix related to the geometric location of Γ_1. The numerical scheme is discussed in detail by Chou (1983).

(2) Current Potential in Region II

The region II has a closed domain. It is bounded by the pseudo-boundary Γ_1 and the boundaries of cylinders Γ_2. The current potential in this region, $\varphi^{(2)}$, satisfies the Laplace equation, can be determined by the following integral equation,

$$
c\,\varphi^{(2)}(x, y) = \frac{1}{2\pi} \int_{\Gamma} \left[\frac{\partial \varphi^{(2)}(\xi, \eta)}{\partial \nu} \ln \frac{1}{r} - \varphi^{(2)}(\xi, \eta) \frac{\partial}{\partial \nu} \left(\ln \frac{1}{r} \right) \right] ds \tag{7}
$$

where $\varphi^{(2)}(\xi, \eta)$ and $\partial \phi^{(2)}(\xi, \eta)/\partial \nu (= \overline{\varphi}^{(2)})$ are the potential and its normal derivative, and $r = \sqrt{(x-\xi)^2 + (y-\eta)^2}$. The factor c is equal to unity within boundaries, but will be $1/2$ on smooth boundaries. As stated before, Eq. (7) can be expressed in a matrix form as the same as Eq. (5),

$$
\left\{ \varphi^{(2)} \right\} = \{k\} \left\{ \overline{\varphi}^{(2)} \right\} \tag{8}
$$

(3) Boundary Conditions of Current Potential

Necessary boundary conditions for the case under consideration are summarized in the following:

1) Free water surface condition: It is assumed that the variations of water level due to the current can be neglected.

$$
\frac{\partial \varphi}{\partial z} = 0, \qquad z = 0 \tag{9}
$$

2) Boundary condition on the impermeable cylinders: For an impermeable cylinders, the flow is null in the normal direction.

$$\frac{\partial \varphi}{\partial \nu} = 0, \qquad \text{on } \Gamma_2 \tag{10}$$

3) Boundary condition on the pseudo-boundary Γ_1: Continuity of mass and energy fluxes between region I and region II at the pseudo-boundary Γ_1 leads to the expressions.

$$\frac{\partial \varphi^{(1)}}{\partial \nu} = \frac{\partial \varphi^{(2)}}{\partial \nu} \tag{11}$$

$$\varphi^{(1)} = \varphi^{(2)} \tag{12}$$

(4) A System of Equations

To facilitate the substitution of boundary conditions, Eq. (8) is first decomposed into two sub-matrices containing contributions from the pseudo-boundary Γ_1, and the boundary of cylinders Γ_2, respectively. Dividing the boundaries into N_1, N_2 constant elements, with the total number of elements equal to N $(= N_1 + N_2)$, Eq. (8) can be expressed as

$$\left\{\varphi_i^{(2)}\right\} = \{k_{ij}\}\left\{\overline{\varphi}_j^{(2)}\right\} \quad (i,j = 1,2) \tag{13}$$

Substituting Eq. (2) into Eqs. (11) and (12) together with Eq. (5), then a little algebra leads to,

$$\left\{\overline{\varphi}_1^{(2)}\right\} = \{k_{11} - k^*\}^{-1}\left\{\varphi^0 - k^*\overline{\varphi}^0\right\} \tag{14}$$

Substituting Eqs. (14) and (10) into Eq. (13), the current potential $\varphi_1^{(2)}$ and $\varphi_2^{(2)}$ on boundaries Γ_1 and Γ_2 can be calculated.

(5) Current Velocities in Region II

As the current potential $\varphi^{(2)}$ and its normal derivative $\overline{\varphi}^{(2)}$ have been obtained, the components of current velocity u and v in region II can be expressed in terms of potential and its normal derivative on the boundaries of region II as,

$$u_i = \frac{1}{2\pi}\sum_{j=1}^{N} \left\{\overline{\varphi}_j^{(2)}\left(\frac{x_j - x_i}{r^2}\right) - \varphi_j^{(2)}\left[\frac{\nu_x}{r^2} - \frac{2(x_j - x_i)[(x_j - x_i)\nu_x + (y_j - y_i)\nu_y]}{r^4}\right]\right\} ds_j \tag{15}$$

$$v_i = \frac{1}{2\pi}\sum_{j=1}^{N} \left\{\overline{\varphi}_j^{(2)}\left(\frac{y_j - y_i}{r^2}\right) - \varphi_j^{(2)}\left[\frac{\nu_y}{r^2} + \frac{2(y_j - y_i)[(x_j - x_i)\nu_x + (y_j - y_i)\nu_y]}{r^4}\right]\right\} ds_j \tag{16}$$

where ν_x and ν_y are, respectively, the components of unit normal vector ν on the boundary in the x- and y-directions, the subscript i denotes the location within region II.

2.2 Wave Potential

A wave is assumed to incident from open sea region far away from cylinders. It has an angular frequency σ_o, an amplitude ζ_o, and a wave number k_o. The wave intersects the x-axis with an angle ω_o. The following linear dispersion relation is assumed to hold,

$$\frac{\sigma_o^2 h}{g} = k_o h \tanh k_o h \tag{17}$$

where g is the gravitational acceleration. It is assumed that the current velocity and the wave motion are small. The wave potential can be expressed as,

$$\Phi^W = \frac{g\zeta_o}{\sigma_o}\,\phi\, e^{-i\sigma t} \tag{18}$$

where $i = \sqrt{-1}$ is the imaginary constant, t is time, ϕ is the dimensionless potential function satisfying the Laplace equation,

$$\frac{\partial^2\phi}{\partial x^2} + \frac{\partial^2\phi}{\partial y^2} + \frac{\partial^2\phi}{\partial z^2} = 0 \tag{19}$$

and σ in Eq. (18) can be expressed as the relation of Doppler effect.

$$\sigma = \sigma_o + \vec{k}\cdot\vec{U} \tag{20}$$

The frequency σ is the apparent wave frequency due to current. In Eq. (20), $|\vec{k}| = k_o$ is wave number, $|\vec{U}| = \sqrt{u_i^2 + v_i^2}$ is current velocity in region II. When both $|\vec{k}|$ and $|\vec{U}|$ have been known, applying the Doppler effect, the apparent wave frequency σ in the wave-current field can be calculated and is then used to the boundary condition of free water surface.

(1) Wave Potential in Region I

The wave potential in region I, $\phi^{(1)}$, is a combination of the potential of incident wave, ϕ^o, and the diffracted wave potential due to the cylinders, ϕ^*,

$$\phi^{(1)}(x,y,z) = \phi^o(x,y,z) + \phi^*(x,y,z) \tag{21}$$

It is assumed that the pseudo-boundary Γ_1 is sufficiently far away from the cylinders, the wave scattering due to them can be neglected in region I. Due to the assumption of constant water depth, h, in region I, potential $\phi^{(1)}$ in region I can be expressed in the following way,

$$\phi^{(1)}(x,y,z) = [f^o(x,y) + f^*(x,y)]\frac{\cosh k_o(z+h)}{\cosh k_o h} \tag{22}$$

where f^o is the incident wave potential function, and f^* is the diffracted wave potential function induced by the presence of cylinders. In the wave-current field, the incident wave potential is written as

$$f^o(x,y)\cdot\exp[-i\sigma t] = -i\cdot\exp\{-i[k_o(x\cos\omega_o + y\sin\omega_o) + \sigma t]\} \tag{23}$$

Substituting Eq. (22) into Eq. (19), one obtains the potential function f^*, which satisfies the Helmholtz equation of the following form.

$$\frac{\partial^2 f^*}{\partial x^2} + \frac{\partial^2 f^*}{\partial y^2} + k_o^2 f^* = 0 \tag{24}$$

On the far-field boundary Γ_∞, f^* must satisfy the Sommerfeld radiation condition,

$$\lim_{r\to\infty} \sqrt{r}\left[\frac{\partial f^*}{\partial r} - ik_o f^*\right] \to 0 \tag{25}$$

where r is the radial ordinate. According to Green's second identity, the potential function f^* in region I can be obtained from the following integral equation,

$$c\, f^*(x,y) = \frac{i}{4}\int_{\Gamma_1}\left\{\overline{f}^*(\xi,\eta)H_o^{(1)}(k_o r) - f^*(\xi,\eta)\frac{\partial}{\partial \nu}[H_o^{(1)}(k_o r)]\right\} ds \tag{26}$$

where $f^*(\xi,\eta)$ is the potential function specified by the geometric condition of the boundaries in region I, $\overline{f}^*(\xi,\eta)(=\partial f^*(\xi,\eta)/\partial\nu)$ is its normal derivative with ν local normal coordinate to boundary taken outwards, and $H_o^{(1)}$ is the zeroth order Hankel function of the first kind. As stated before, the factor c equals to unity within the boundary but will have a value of $1/2$ on smooth boundaries. For the case that $c = 1/2$, Eq. (26) can be discretized in a matrix form as follows,

$$\{F^*\} = \{K^*\}\left\{\overline{F}^*\right\} \tag{27}$$

where

$$\left.\begin{aligned}
\{F^*\} &= f_j^* \quad , \quad j = 1,2,\cdots,N_1 \\
\left\{\overline{F}^*\right\} &= \overline{f}_j^* \\
\{K^*\} &= \{H^*\}^{-1}\{G^*\} \\
\{H^*\} &= H_{ij}^* \quad , \quad i,j = 1,2,\cdots,N_1 \\
\{G^*\} &= G_{ij}^* \\
H_{ij}^* &= \begin{cases} \overline{H}_{ij}^* & (i \neq j) \\ \overline{H}_{ij}^* + \dfrac{1}{2} & (i = j) \end{cases} \\
\overline{H}_{ij}^* &= \frac{i}{4}\int_{\Gamma_j}\frac{\partial}{\partial\nu}[H_o^{(1)}(k_o r)]ds \\
G_{ij}^* &= \frac{i}{4}\int_{\Gamma_j} H_o^{(1)}(k_o r)ds
\end{aligned}\right\} \tag{28}$$

in which $\{F^*\}$ and $\left\{\overline{F}^*\right\}$ are the potential function and its normal derivative on pseudo-boundary Γ_1, respectively, and $\{K^*\}$ is the coefficient matrix related to the geometric location of Γ_1. The numerical scheme is discussed in detail by Chou (1983).

(2) Wave Potential in Region II

Region II is a closed three-dimensional domain with constant water depth. It is bounded by the pseudo-boundary, S_1, the free water surface, S_2, the surfaces of impermeable cylinders, S_3, and an impermeable sea bed, S_4. Expressing $S = S_1 + S_2 + S_3 + S_4$, and taking that the potential function for the waves in region II, $\phi^{(2)}$, must satisfy the Laplace equation, then according to Green's second identity law, velocity potential $\phi^{(2)}(x, y, z)$ for any point within region II can be determined by the velocity potential on the boundary, $\phi^{(2)}(\xi, \eta, \zeta)$, together with its first normal derivative, $\overline{\phi}^{(2)}(\xi, \eta, \zeta)$, that is,

$$c\,\phi^{(2)}(x, y, z) = \frac{1}{4\pi}\int_S \left[\overline{\phi}^{(2)}(\xi,\eta,\zeta)\frac{1}{R} - \phi^{(2)}(\xi,\eta,\zeta)\frac{\partial}{\partial\nu}\frac{1}{R}\right] dA \tag{29}$$

where $R = \sqrt{(x-\xi)^2 + (y-\eta)^2 + (z-\zeta)^2}$. As stated before, c is unity for points inside the region and is equal to $1/2$ on the boundaries.

To proceed with numerical calculation, the surfaces of boundaries S_1 through S_4, are divided into N_1 to N_4 discrete segments with constant plane element, respectively. For the case that $c = 1/2$, Eq. (29) is readily expressed as,

$$\left\{\phi^{(2)}\right\} = \{K\}\left\{\overline{\phi}^{(2)}\right\} \tag{30}$$

where

$$\left.\begin{aligned}
\left\{\phi^{(2)}\right\} &= \phi_j^{(2)}\ ,\ j = 1, 2, \cdots, N_1 + N_2 + N_3 + N_4 \\
\left\{\overline{\phi}^{(2)}\right\} &= \overline{\phi}_j^{(2)} \\
\{K\} &= \{H\}^{-1}\{G\} \\
\{H\} &= H_{ij}\ ,\ j = 1, 2, \cdots, N_1 + N_2 + N_3 + N_4 \\
\{G\} &= G_{ij} \\
H_{ij} &= \begin{cases} \overline{H}_{ij} & (i \neq j) \\ \overline{H}_{ij} + \dfrac{1}{2} & (i = j) \end{cases} \\
\overline{H}_{ij} &= \frac{1}{4\pi}\int_{A_j} \frac{\partial}{\partial\nu}\frac{1}{R} dA \\
G_{ij} &= \frac{1}{4\pi}\int_{A_j} \frac{1}{R} dA
\end{aligned}\right\} \tag{31}$$

where $\left\{\phi^{(2)}\right\}$ and $\left\{\overline{\phi}^{(2)}\right\}$ are the potential fuction and its normal derivative on the boundary S, and $\{K\}$ is a coefficient matrix related to the geometry of the boundaries. The numerical scheme is discussed in detail by Chou (1983).

Neglecting the hydrostatic pressure and substituting Eqs. (1) and (18) into Eq. (42), the total wave force on each cylinder can be calculated by the dynamic pressure with integration over the surface of each cylinder.

$$F = \frac{\rho g \zeta_o}{\sigma_o} e^{-i\sigma t} \int [-i\sigma\phi^{(2)} + \nabla\varphi^{(2)} \cdot \nabla\phi^{(2)}] \nu \, dA \tag{44}$$

From Eq. (18), the wave height ratio, K_d $(= \zeta/\zeta_o)$, is given by

$$K_d = \frac{1}{\sigma_o} |i\sigma\phi - \nabla\varphi^{(2)} \cdot \nabla\phi^{(2)}| \tag{45}$$

III. NUMERICAL RESULTS AND DISCUSSION

On a uinform current field, waves are affected by the relative magnitude of the current velocity. For example, the waves propagating against the current will be forced to halt when the current has a velocity,

$$U_o \geq -\frac{C_o}{4} \tanh k_o h \tag{46}$$

where C_o is the wave velocity.

For the purpose to satisify above condition, $F_r = 0.1$ is taken. The incident angle of waves is $\omega_o = 0°$, wave number $k_o h$ is varied from 0.1 to 1.6, and the angles θ_o $(= \beta_o - \omega_o) = 0°$, 45°, 90°, 135° and 180° are used. The radius of cylinder, a, is $0.25h$, and the distance between cylinders, D_s, is $0.25h$.

3.1 Wave Force

Figure 2(a) presents the wave force of x-component on single cylinder. As shown in Fig. 2(a), the wave force decreases with an increase in θ_o for $k_o h$ less than 1.2. For the cases of $\theta_o = 0°$ and 45°, the wave force is larger than those in absence of current, but for the cases of $\theta_o = 135°$ and 180°, it becomes smaller. Figure 2(b) shows the wave force on cylinder of y-component, which is very small and less than 0.015.

Figure 3 shows the x- and y-components of the wave force on each cylinder for the case of double cylinders. The variation of x-component of wave force with wave number is similar to the single cylinder. The y-component of wave force on cylinder is shown in Fig. 3(c) and 3(d), it is larger due to the distribution of asymmetrical pressure around cylinder for any angles θ_o . For the cases of $\theta_o = 0°$ and 45°, the y-component is larger than those in absence of current, but for the cases of $\theta_o = 135°$ and 180°, the wave force on each cylinder is less than those in absence of current for the wave number $k_o h$ larger than 0.7.

Figure 4 shows the x- and y-components of wave force on each cylinder for the triple cylinders. The variation of wave force with wave number on each cylinder are similar to the single or double cylinders. The x-component of wave force on the middle cylinder (No. 1) is larger than the others (No. 2 and No. 3), but the y-component is less than the others.

Figure 5 compares the x- and y-components of wave force on cylinder for the triple cylinders with $\theta_o = 45°$, 90° and 135°. It is demonstrated that the x-component of wave force on cylinder of No. 2 and No. 3 is almost equal, excepting $k_o h > 1.0$.

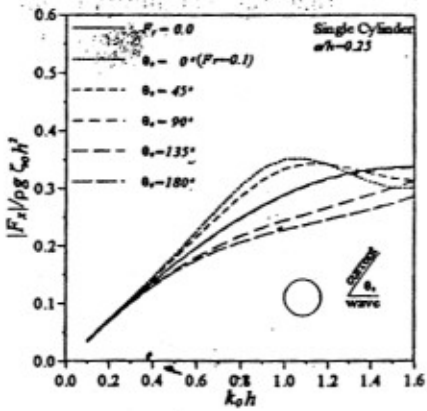

(a) x-component

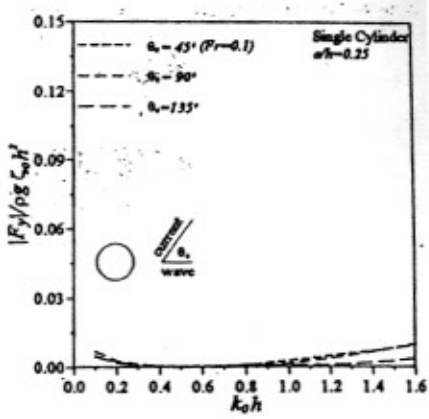

(b) y-component

Fig. 2 Wave force of single cylinder.

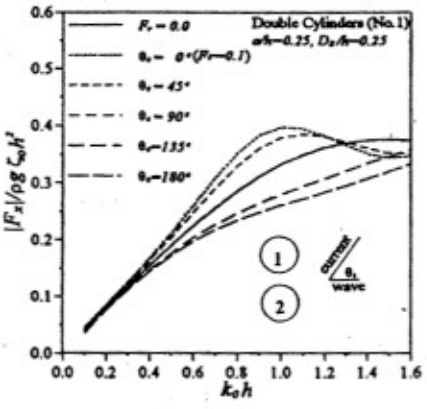

(a) x-component of No. 1 cylinder

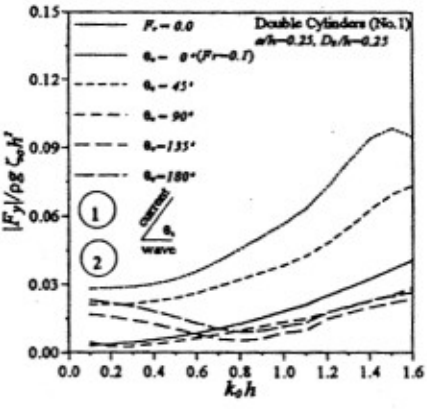

(c) y-component of No. 1 cylinder

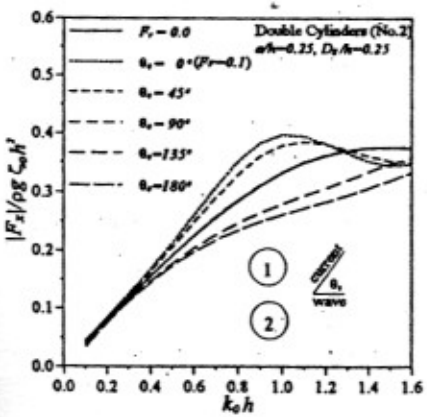

(b) x-component of No. 2 cylinder

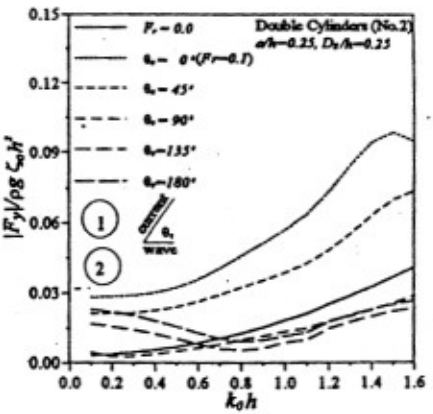

(d) y-component of No. 2 cylinder

Fig. 3 Wave force of dluble cylinders.

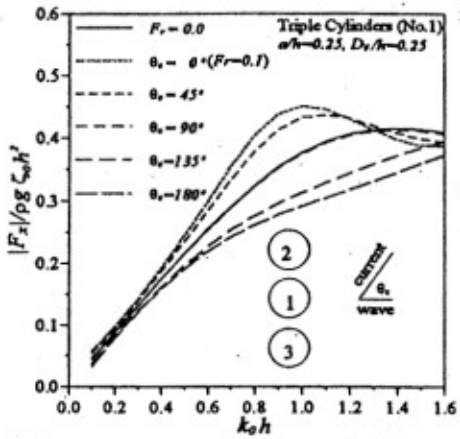

(a) x-component of No. 1 cylinder

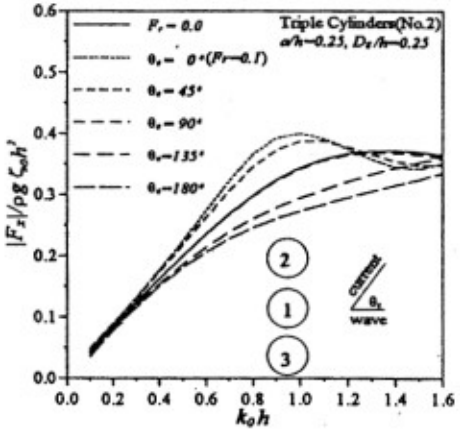

(b) x-component of No. 2 cylinder

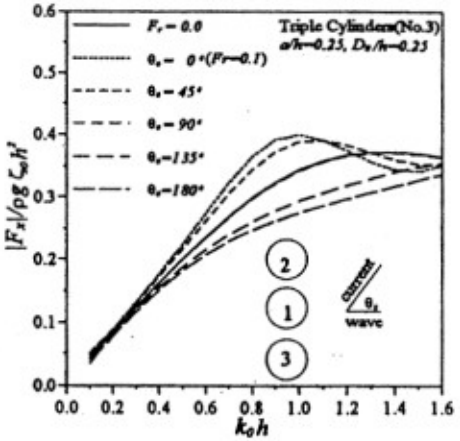

(c) x-component of No. 3 cylinder

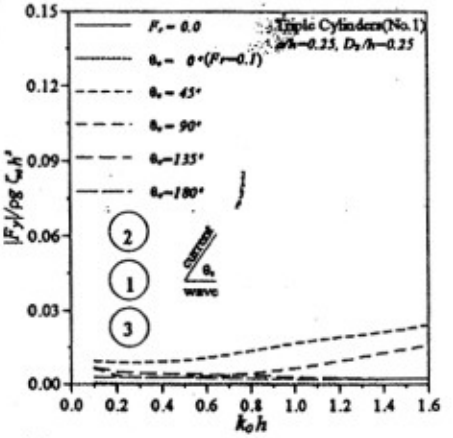

(d) y-component of No. 1 cylinder

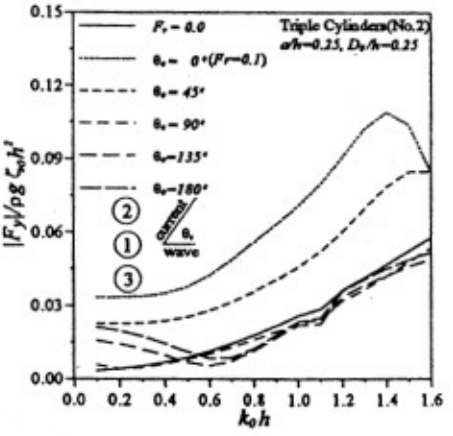

(e) y-component of No. 2 cylinder

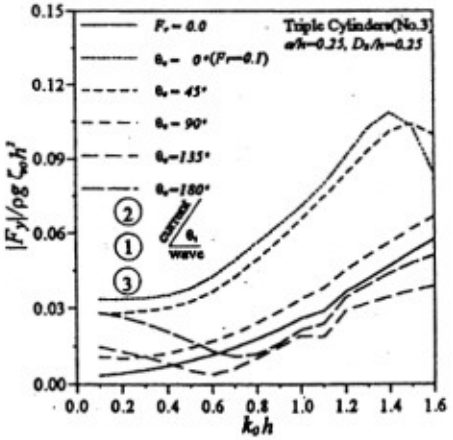

(f) y-component of No. 3 cylinder

Fig. 4 Wave force of triple cylinders.

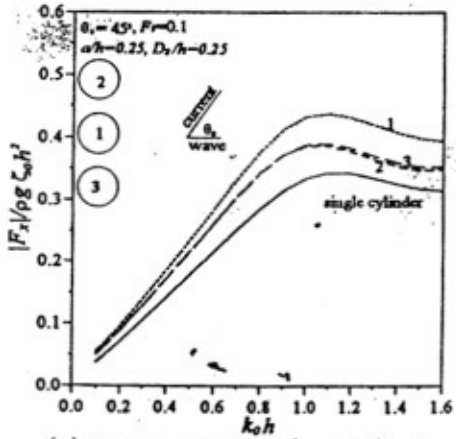

(a) x-component at $\theta_0 = 45°$

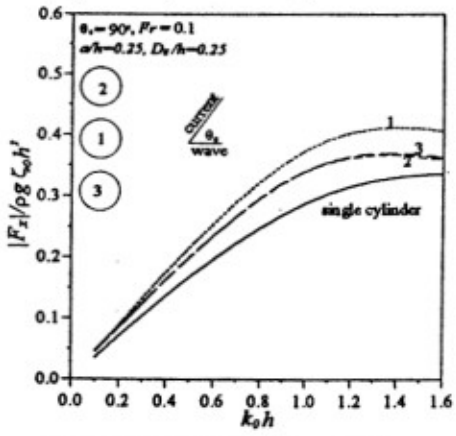

(b) x-component at $\theta_0 = 90°$

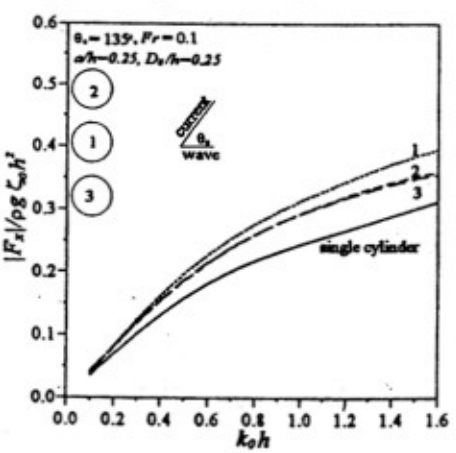

(c) x-component at $\theta_0 = 135°$

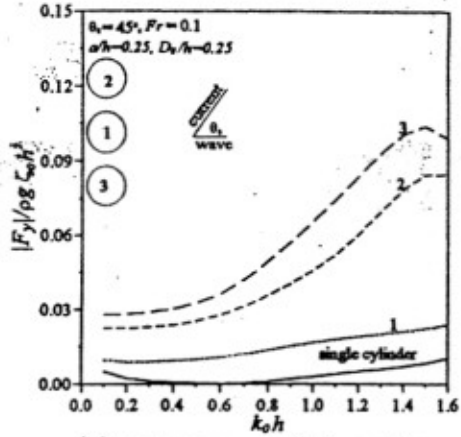

(d) y-component at $\theta_0 = 45°$

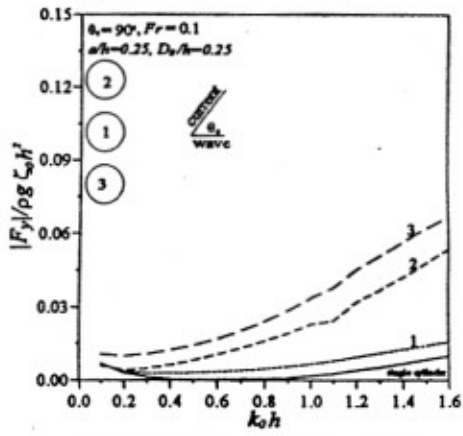

(e) y-component at $\theta_0 = 90°$

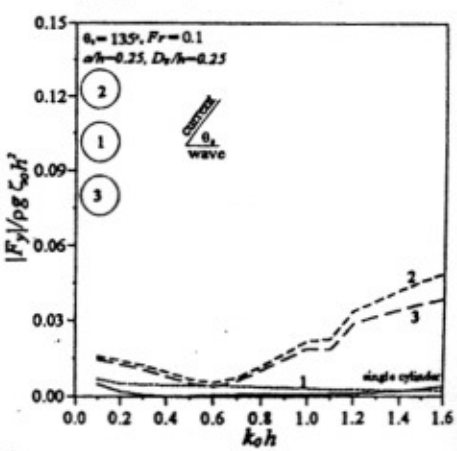

(f) y-component at $\theta_0 = 135°$

Fig. 5 Comparisons for wave force of x, y-component with different angles.

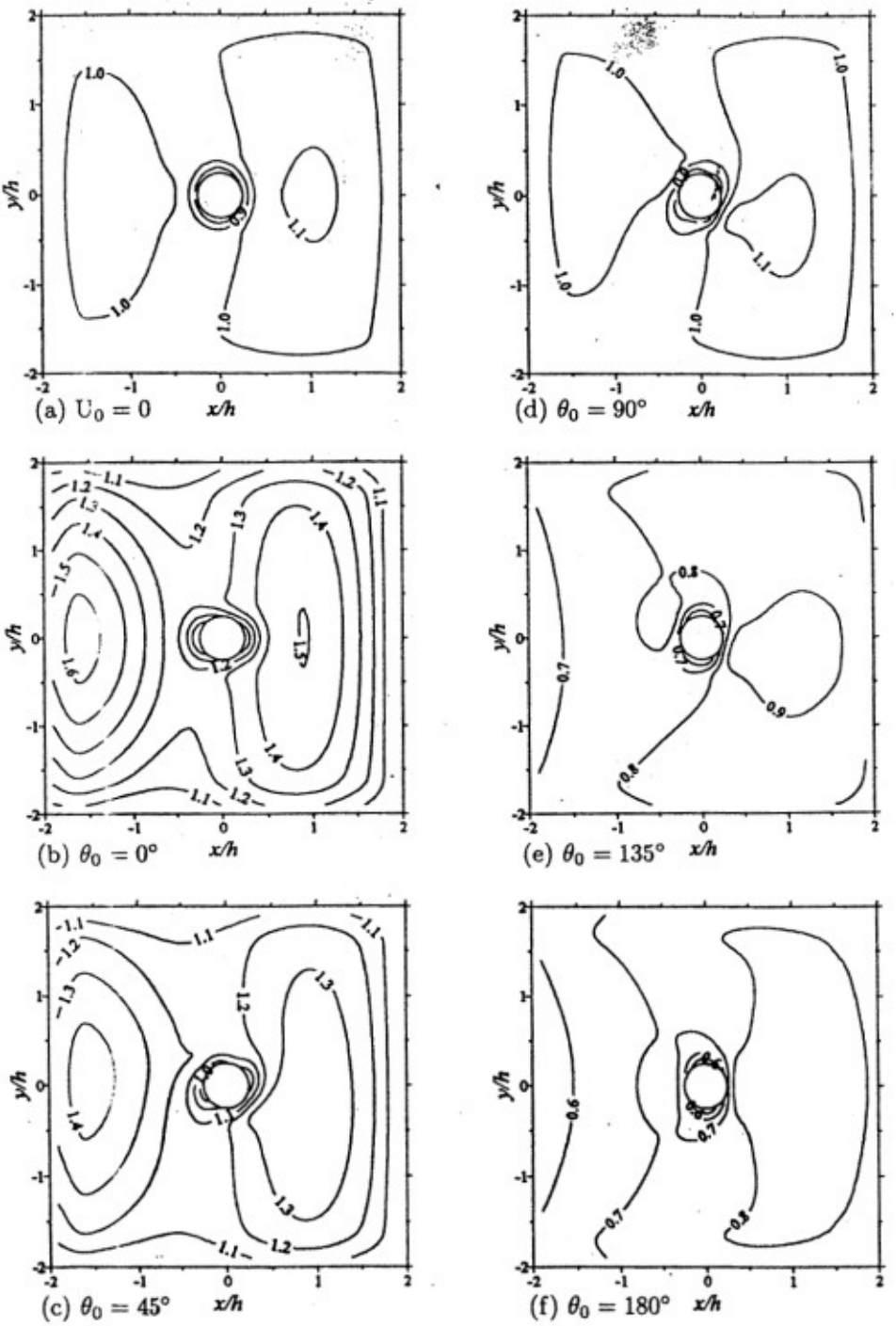

Fig. 6 Wave height distributions for single cylinder, $k_0h = 1.0$, $\omega_0 = 0°$, $a/f = 0.25$ and $F_r = 0.1$

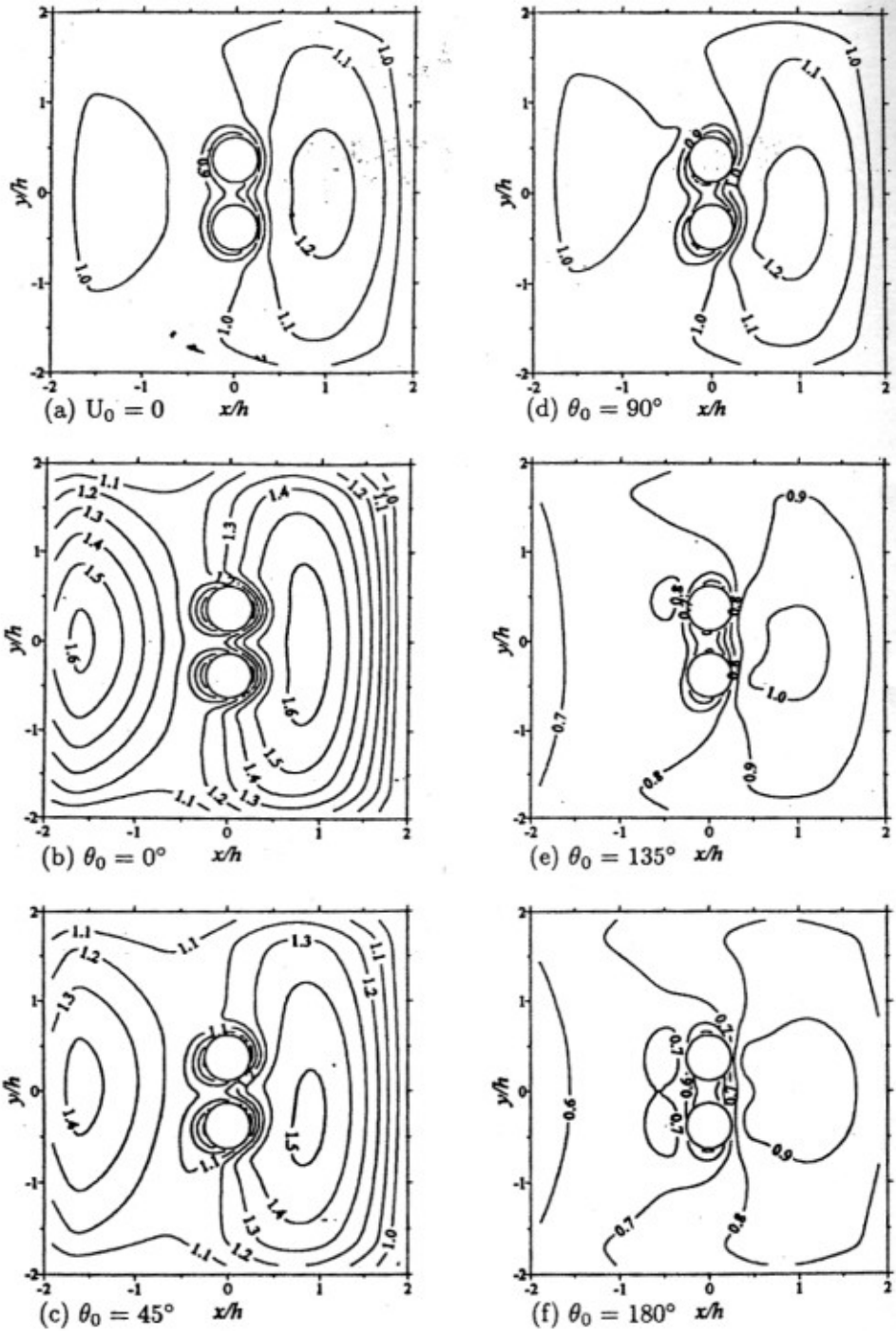

Fig. 7 Wave height distributions for double cylinders, $k_0 h = 1.0$, $\omega_0 = 0°$, $a/f = 0.25$, $D_s = 0.25$ and $F_r = 0.1$

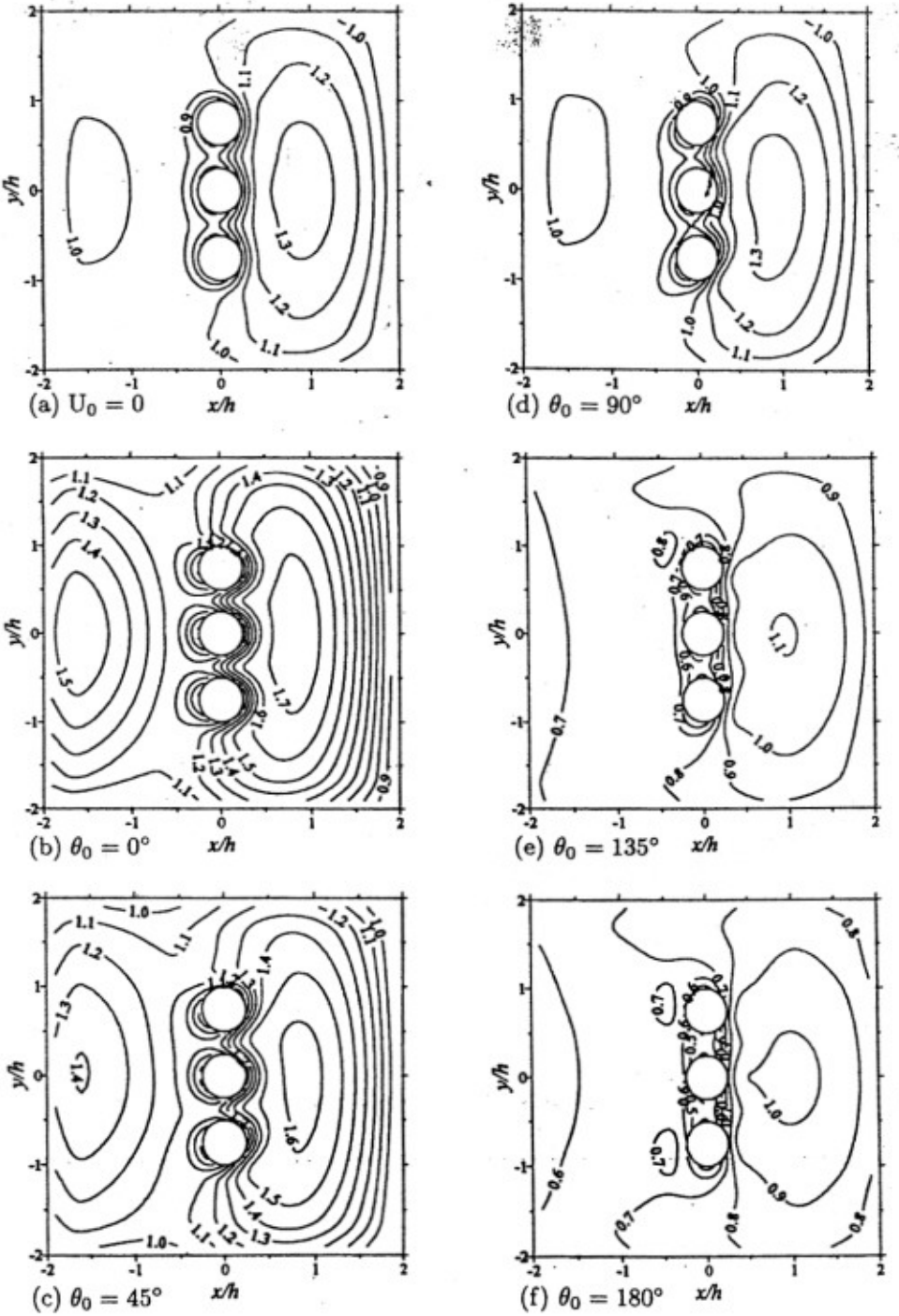

Fig. 8 Wave height distributions for triple cylinders, $k_0h = 1.0$, $\omega_0 = 0°$, $a/f = 0.25$, $D_s = 0.25$ and $F_r = 0.1$

For the cases of $\theta_o = 45°$ and $90°$, the cylinder of No. 3 has the largest force of y-component and the smallest one is cylinder of No. 1, but for the case of $\theta_o = 135°$, the y-component of No. 2 is the largest one.

3.2 Distribution of Wave Height

Figures 6-8 show the wave height distributions for $k_o h = 1.0$ ($\sigma_o^2 h/g = 0.762$) and the angle of incident wave is $\omega_o = 0°$.

Figure 6(a), shows the case of single cylinder in wavefield without current, the distributions of wave height are symmetrical to the direction of incident wave. As shown in Fig. 6(b), the wave heights are increased, because wave propagates in the same direction as current. The distributions of wave height also symmetrize about the x-axis. Figure 6(c) shows the case of $\theta_o = 45°$, the wave heights are unevenly distributed and shifted toward the negative y-direction due to the Doppler effect. Figure 6(d) shows the case of $\theta_o = 90°$, the distributions of wave height are similar to those in absence of current, besides those have a little asymmetry about the direction of incident wave. It is caused by the wave numbers $|\vec{k}|$ at any place on water surface are variously due to the Doppler effect. For the cases of $\theta_o = 135°$ and $180°$, the wave heights decrease as shown in Fig. 6(e) and 6(f) due to the current propagating against the wave.

Figure 7 and 8 show the distributions of wave height for the cases of double and triple cylinders in wave-current field. The variety of distributions of wave height is similar to that of single cylinder.

IV. CONCLUSION

First of all in this paper, the two-dimensional boundary element method is applied to obtain the distribution of current field. Secondly, the Doppler effect is used to express the dispersion relation of wave which includes the effect of current. The Doppler effect takes it into the boundary condition of free water surface. Finally, the three-dimensional boundary element is applied to obtain the velocity potential in wave-current field which is affected by the cylinders.

According to our method, the interaction among current, wave and cylinders can be properly expressed, even for the case of the direction between wave and current are perpendicular.

ACKNOWLEDGMENT

The financial support of this project by the National Science Council of the Republic China is hereby acknowledged. Project No. NSC-83-0209-E-019-002.

REFERENCES

Baddour, R. E. and S. Song (1990): On the interaction between waves and currents, Ocean Engineering, Vol. 17, No. 1/2, pp. 1–21.

Chou, C. R. (1983), Application of Boundary Element Method to Wave Dynamics, Institute of Department of Harbor and River Engineering, Taiwan Ocean University, Keelung, Taiwan, pp. 92–98, pp. 135–143, pp. 148–150.

Chou, C. R. and W. Y. Han (1993): Wave-induced oscillations in harbours with dissipating quays, Coastal Engineering in Japan, Vol. 36, No. 1, pp. 1–23.

Eatock Taylor, R., C. S. Hu and F. G. Nielsen (1990): Mean drift forces on a slowly advancing vertical cylinder in long waves, Appl. Ocean Res., Vol. 12(3), pp. 141–152.

Grue, J. and E. Palm (1985): Wave radiation and wave diffraction from a submerged body in a uniform current, Journal of Fluid Mechanics, Vol. 151, pp. 257–278.

Isaacson, M. and K. F. Cheung (1993): Time-domain solution for wave-current interaction with a two-dimensional body, Appl. Ocean Res., Vol. 15, pp. 39–52.

Longuet-Higgins, M. S. and R. W. Stewart (1961): The changes in amplitude of short gravity waves on steady non-uniform currents, Journal of Fluid Mechanics, Vol. 10, pp. 529–549.

Matsui, T., S. Y. Lee and K. Sano (1991): Hydrodynamic forces on a vertical cylinder in current and waves, Journal of the Society of Naval Architects of Japan, No. 170, pp. 277–287.

Newman, J. N. (1978): The theory of ship motions, Advances in Applied Mechanics, Vol. 18, pp. 221–282.

Peregrine, D. H. (1976): Interaction of water wave and currents, Advances in Applied Mechanics, Vol. 16, pp. 9–117.

Thomas, G. P. (1981): Wave-current interactions: an experimental and numerical study, Part 1. Linear waves, J. Fluid Mech., Vol. 110, pp. 457–474.

Zhao, R. and O. M. Faltinsen (1988): Interaction between waves and current on a two-dimensional body in the free surface, Appl. Ocean Res., Vol. 10(2), pp. 87–99.

(Received May 27, 1996; Revised Aug. 7, 1996)